Journal of Asian Ceramic Societies

ISSN: (Print) 2187-0764 (Online) Journal homepage: https://www.tandfonline.com/loi/tace20

Synthesis of high density sub-10 μm $(Ba_{0.85}Ca_{0.15})(Zr_{0.1}T_{i0.9})O_3$-$xCeO_2$ lead-free ceramics using a two-step sintering technique

Vijay Bijalwan & Pavel Tofel

To cite this article: Vijay Bijalwan & Pavel Tofel (2019) Synthesis of high density sub-10 μm $(Ba_{0.85}Ca_{0.15})(Zr_{0.1}T_{i0.9})O_3$-$xCeO_2$ lead-free ceramics using a two-step sintering technique, Journal of Asian Ceramic Societies, 7:4, 536-543, DOI: 10.1080/21870764.2019.1683954

To link to this article: https://doi.org/10.1080/21870764.2019.1683954

Published online: 29 Oct 2019.

JOURNAL OF ASIAN CERAMIC SOCIETIES
2019, VOL. 7, NO. 4, 536–543
https://doi.org/10.1080/21870764.2019.1683954

THE CERAMIC SOCIETY OF JAPAN
THE KOREAN CERAMIC SOCIETY
Taylor & Francis
Taylor & Francis Group

FULL LENGTH ARTICLE

Synthesis of high density sub-10 µm $(Ba_{0.85}Ca_{0.15})(Zr_{0.1}T_{i0.9})O_3$-x$CeO_2$ lead-free ceramics using a two-step sintering technique

Vijay Bijalwan [a,b] and Pavel Tofel [a,c]

[a]Advanced Materials, CEITEC—Central European Institute of Technology, Brno, Czech Republic; [b]Department of Ceramics, and Polymers, Faculty of Mechanical Engineering, Brno University of Technology, Brno, Czech Republic; [c]Department of Physics, Faculty of Electrical Engineering and Computer Science, Brno University of Technology, Brno, Czech Republic

ABSTRACT

$(Ba_{0.85}Ca_{0.15})(Zr_{0.1}T_{i0.9})O_3$-x$CeO_2$, (BCZTCe) lead-free piezoelectric ceramics were processed conventionally using a two-step sintering technique. The results suggest that two-step sintering is an effective technique to acquire a high density (99%) homogeneous microstructure with sub-10 µm grain size. The low CeO_2 content (0.07 wt.%) facilitates good functional properties at low sintering conditions of T_1 = 1400°C/30 min & T_2 = 1275°C/4 h, in which d_{33} = 353 ± 7 pC/N, k_p= 40%, ε_r= 3393 ± 100, *tan* δ =0.039, T_C = 96.5°C, P_r = 11.45 µC/cm^2, E_C = 2.32 kV/cm and a large strain of 0.18%. These results indicate that BCZTCe ceramics are a promising lead-free piezoelectric substitute for room temperature device applications.

ARTICLE HISTORY
Received 25 July 2019
Accepted 8 October 2019

KEYWORDS
Lead free ceramics; d_{33}; two-step sintering; high density; microstructure

1. Introduction

Piezoelectric materials are smart functional materials that can convert energy (mechanical to electrical or vice versa) and are used in a variety of electronic devices [1–4]. Among these lead zirconate titanate (PZT) and related materials are dominant in terms of use of their piezoelectric properties in sensors, actuators, fuel injectors, transducers, etc [1,3]. Due to the lead (Pb) toxicity and its non-environmentally friendly nature, a search has begun to replace PZT and related systems [3,4]. Lead-derived materials exhibit a morphotropic phase boundary (MPB), which generates enhanced ferroelectric and piezoelectric properties. Hence, work on lead-free systems has also concentrated on developing systems with an MPB.

$(Ba_{0.85}Ca_{0.15})$ $(Zr_{0.1}T_{i0.9})$ O_3 (BCZT) lead-free material system developed by Liu and Ren in 2009 showed excellent piezoelectric properties: d_{33} ~ 620 (pC/N [5]. Several groups have tried to reproduce these results since then but could not achieve the same results with pure BCZT and other solid solutions (d_{33} < 470 pC/N) [6–11]. A possible reason behind their inferior results may be the stoichiometric ratio, method of synthesis and sintering techniques used for the preparation of raw powders and the final sintered body. The method used in previous publications does not guarantee stoichiometric homogeneity during processing, which can cause fluctuation of the piezoelectric properties. These techniques include the solid-state reaction method [12], hot pressing method [13], modified pechini method [14] and the application of various processing parameters such as calcination temperatures [15]. Piezoelectric constants fluctuate as 500–650 (pC/N) from these methods which is mainly due to fluctuations in the initial particle size, density and pore size distribution.

Previous reports indicate that the grain size can greatly affect dielectric and piezoelectric responses in piezoceramics [16–19]. To reduce the sintering temperature of BCZT ceramics, different dopants were used as sintering aids, while maintaining good piezoelectric properties [20–23]. Grain-size deviations can also cause variability in the functional properties [24,25].

There are always experimental complications in synthesizing a series of dense $BaTiO_3$ (BT) based lead-free ceramics with different desired values such as an average grain size using a sole source of BT powder as well as a single sintering technique [26]. Accordingly, different kinds of BT powder and sintering techniques have usually been combined, such as those described by Arlt et al. [27]. This may distress the consistency of the experimental results owing to the different characters of the obtained BT ceramics. To this approach, it is highly desirable in studying grain-size effects (sub-10 µm) to use a group of BT ceramics (Such as BCZT) that offers a very high final ceramic density and a uniform grain-size distribution in their microstructures in order to obtain good functional properties, in particular.

The present study is a follow-up to our previous study in which we prepared $(Ba_{0.85}Ca_{0.15})$ $(Zr_{0.1}T_{i0.9})$ O_3 – xCeO_2 ceramics by the conventional method and conventional single-step sintering [28]. In that study, we found that a grain size of ~13 µm and density of ~95% were suitable for obtaining high piezoelectric

CONTACT Vijay Bijalwan vijay.bijalwan@ceitec.vutbr.cz CEITEC—Central European Institute of Technology, Purkyňova 123, Brno, Czech Republic

properties (d_{33} > 500 pC/N) at a lower sintering temperature of 1350°C/4 h while doping with CeO_2 [26]. Nonetheless, reports showing the effects of sub-10 μm grain sizes on the functional properties of $(Ba_{0.85}Ca_{0.15})(Zr_{0.1}T_{i0.9})O_3$ ceramics are rare. However, reducing the grain size (<10 μm) while maintaining fairly good properties for BCZT ceramics is a challenge [29,30]. Thus, a two-step sintering technique was introduced in order to further reduce the grain size of these ceramics and study the effects on their functional properties. The main aim of the current study is to maintain grain size (<10 μm) with a homogeneous microstructure and obtain very high-density ceramics together with good piezoelectric, dielectric and ferroelectric properties. $(Ba_{0.85}Ca_{0.15})(Zr_{0.1}T_{i0.9})O_3 - xCeO_2$ (x = 0, 0.02, 0.04, 0.07 wt.%) were prepared using a two-step sintering (TSS) technique. The microstructural, piezoelectric, dielectric and ferroelectric properties were systematically studied.

2. Experimental

$(Ba_{0.85}Ca_{0.15})(Zr_{0.1}Ti_{0.9})O_3 - xCeO_2$ (x = 0, 0.02, 0.04, 0.07 wt.%) materials were processed by the conventional solid-state reaction route. Raw materials of $BaCO_3$ (Dakram, Great Britain, 99.9%) $CaCO_3$ (Lachner, Czech Republic, 99.9%), ZrO_2 (Dakram, Great Britain, 99.9%), TiO_2 (Dakram, Great Britain, 99.9%) and CeO_2 (Sigma Aldrich, Great Britain, 99.9%) were dried in an oven (Lenton MMD/0229, England) at 220°C/1 h before weighing. The raw powders were then mixed with a horizontal ball mill using zirconia milling media and deionized water for 24 h. The resulting slurry was dried in the oven at 90°C for 15 h and then calcined in a muffle furnace (Lenton, 5696, England) at 1250°C for 2 h. Different concentrations of CeO_2 (0–0.07 wt.%), were added in four batches (30 gm each) of the calcined BCZT powders and re-milled in deionized water for 24 h. Approximately 5 wt.% of each binder, Duramax B1000 (Product No. 74821, Chesham Chemicals Ltd., UK), B1007 (Product No. 74823, Chesham Chemicals Ltd., UK) were added during the last hour of milling. The particle sizes were measured using a particle size analyzer (Gracell, Sympa Tec, Germany) and the average particle sizes of all batches were ~2 μm. Dried powder was then sieved (300 mesh, VWR, England) and uniaxially pressed at 155 MPa (Instron, 5507, England) into the green bodies using a 13 mm diameter cylindrical steel die (P.T. No. 3000, Specac, UK). The green bodies were finally sintered at different temperatures using a two-step sintering technique (TSS). In the first step the furnace is programmed for a rapid ramp-up rate 10°C/min to a set temperature T_1 (1350, 1400, 1450°C) with 30 min dwell in order to ensure the uniformity of the heat atmosphere inside the furnace chamber. The furnace was then cooled rapidly at 30°C/min to a lower temperature T_2. This temperature was set at 1275°C to prevent further grain growth and maintained for 4 h. Finally, the temperature was ramped down to room temperature at a rate of 10°C/min. The relative densities were measured by the Archimedes method using the theoretical density (5.80 g/cm^3) from XRD results. The phase structure of the sintered discs was examined by X-ray diffraction (Equinox 3000, INEL, France) with Cu-Kα radiation (λ = 1.54178 Å). A chromium (Cr) – gold (Au) coating was sputtered as electrodes using a sputter coater (K575X, Emitech, UK), and the samples were poled in silicon oil at 3 kV/mm for 10 min. The dielectric properties were measured with an impedance analyzer (4294, Agilent, USA) at 1 kHz. The piezoelectric constant was measured with a Berlincourt d_{33} meter (YE2730A, Sinocera, China). The surface morphologies were observed by scanning electron microscopy (JEOL 6060LV, England). Ferroelectric P-E and S-E hysteresis were measured with an aixACCT Systems (GmbH, Germany) at 1 Hz.

3. Results and discussions

3.1. Microstructures, density and grain size of the samples

The microstructures of all samples of sintered BCZT-$xCeO_2$ ceramics were observed by SEM under sintering conditions of T_1-1400°C/30 min and T_2-1275°C/4 h as shown in Figure 1. All the CeO_2 concentrations were added in wt.% to the BCZT ceramics. It is evident that CeO_2 incorporation up to x = 0.07% causes high densification and uniform microstructures. As the sintering temperature increased further (T_1 = 1450°C/30 min), the samples with x = 0–0.04% became somewhat denser but sample x = 0.07% started to become porous, as seen in Figure 2. From that point on, we designated the *optimum sintering conditions*, i.e. T_1-1400°C/30 min and T_2-1275°C/4 h, as the temperatures at which the maximum relative density with a uniform microstructure were obtained.

The relative densities of BCZT-$xCeO_2$ ceramics treated under different sintering conditions are shown in Figure 3(a), which is in agreement with the microstructural analysis. As the Ce concentration increases, the relative density increases, and is achieved maximum (99%) of theoretical density (t.d. = 5.80 g/cm^3 calculated from cell parameters), for sample x = 0.07 wt.%, under *optimum sintering conditions*, T_1-1400°C/30 min and T_2-1275°C/4 h. For pure BCZT (x = 0) however, a low relative density was observed (~94% of t.d.), even under higher sintering conditions. i.e. T_1-1450°C/30 min and T_2-1275°C/4 h. This clearly suggests that CeO_2 is an effective dopant for achieving high densification of BCZT ceramics at low temperature. The grain size calculations were conducted by the linear intercept method, as shown in Figure 3(b). The average grain size was observed to be ~8 μm for all the samples under different sintering conditions, indicating that the TSS technique could be useful in grain-size reduction

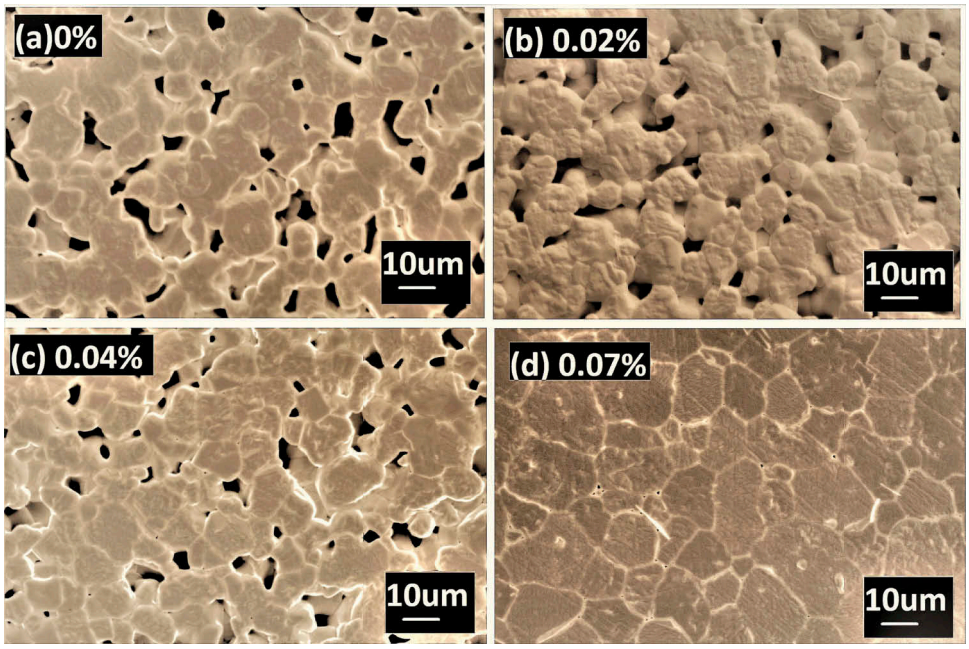

Figure 1. SEM microstructure of BCZT-xCeO_2 ceramics at sintering conditions of T_1-1400°C/30 min & T_2-1275°C/4 h.

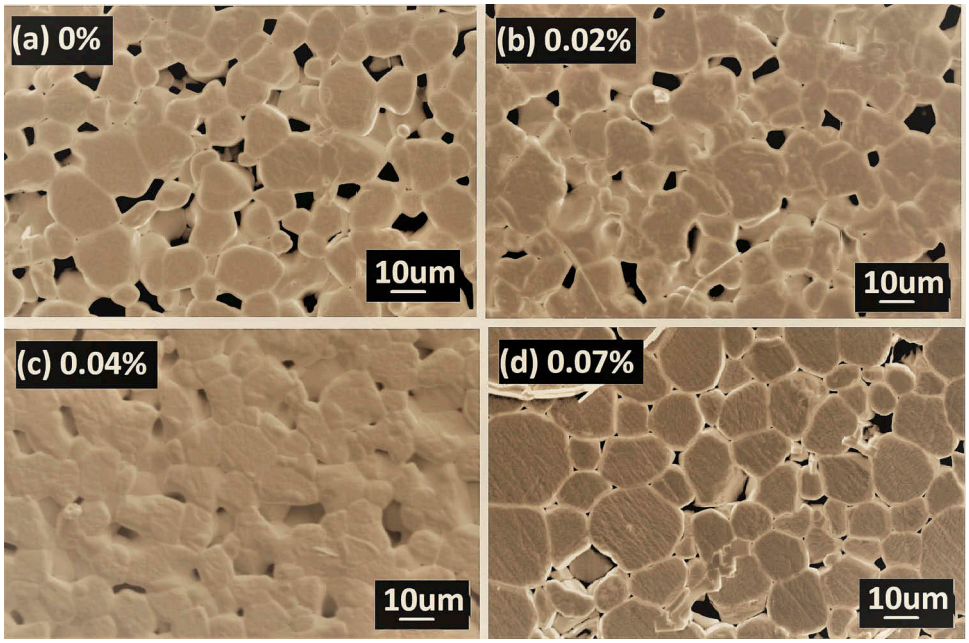

Figure 2. SEM microstructure of BCZT-xCeO_2 ceramics at sintering conditions of T_1-1450°C/30 min & T_2-1275°C/4 h.

and maintenance of a uniform microstructure. The average grain size for x = 0.07% under sintering conditions of T_1-1400°C & T_2-1275°C was 7.96 µm, which is slightly higher than that of such other lead-free piezoelectric materials as KNN and BNT (<3 µm) [4,31,32] but relatively lower than that of pure BCZT (grain size 8 µm) with almost 100% densification [33,34].

3.2. X-ray diffraction analysis and temperature-dependent relative permittivity

Figure 4(a) shows the X-ray diffraction patterns of BCZT-xCeO_2 ceramics produced under optimum sintering conditions of T_1-1400°C & T_2-1275°C in the range of 20°-80°measured at room temperature (21°C). A pure perovskite crystal structure with no trace of a secondary phase was detected indicating that the CeO_2 ions had diffused into the BCZT lattice and formed a solid solution. The distinct sharp XRD peaks denote good homogeneity and crystallinity of the samples. For phase detection, further investigation of the XRD data was conducted by enlarging the 2θ angle between 44°-46° and 83°-85° as shown in Figure 4(b) & 4(c). The splitting of the (200) peak into (002)/(200) reflections at around 45° as well as a single peak (222) reflection at around 83.5° suggest single tetragonal phases (T) for all samples

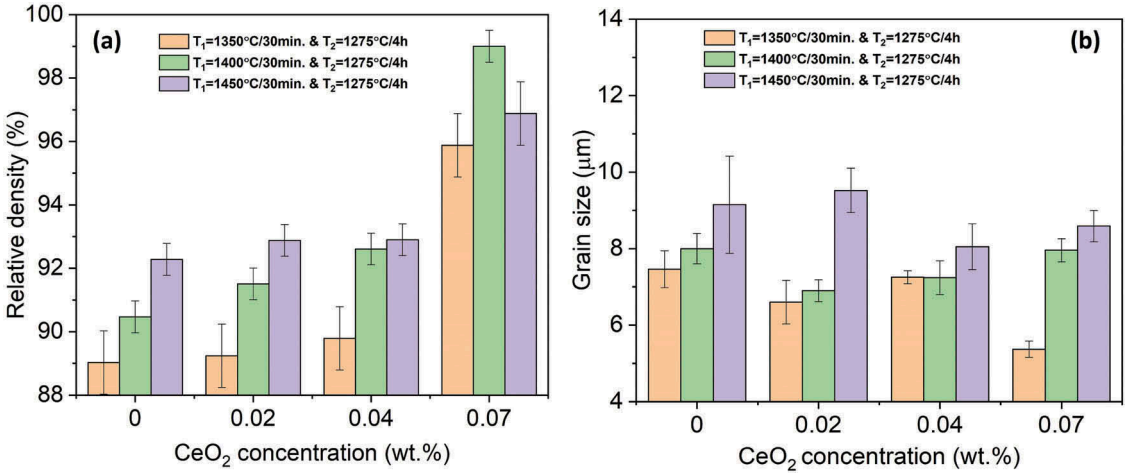

Figure 3. Relative densities and (b) grain sizes of BCZT-xCeO_2 ceramics at different sintering conditions.

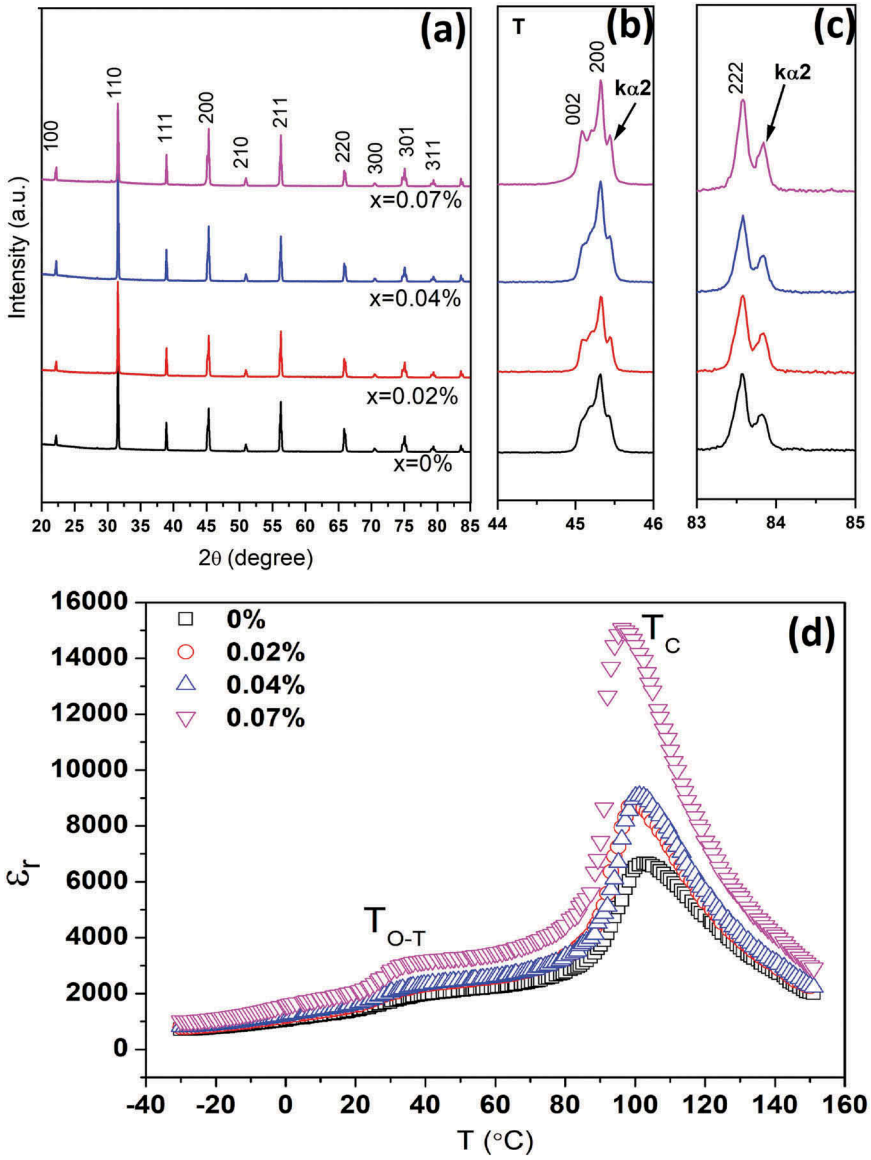

Figure 4. (a) XRD patterns between 20°-80°, (b) enlarged view of 2θ between 44°-46°, (c) enlarged view of 2θ between 83°-85° and (d) plot of dielectric permittivity with respect to temperatures of BCZT-xCeO_2 ceramics at sintering conditions of T_1-1400°C/30 min & T_2-1275°C/4 h min & T_2-1275°C/4 h.

Table 1. Cell parameters of BCZT-xCeO_2 ceramics at sintering conditions T_1-1400°C/30 min and T_2-1275°C/4 h.

BCZT – $_xCeO_2$	a (Å)	c (Å)	Volume (cm^3)	c/a
0	3.998	4.012	64.138	1.0035
0.02	3.998	4.013	64.148	1.0037
0.04	3.998	4.014	64.168	1.0040
0.07	3.998	4.016	64.192	1.0045

provided by Rietveld analysis. All the reflections show an additional peak on the right side of the peaks corresponding to the Kα2 reflection. It was therefore concluded that the low CeO_2 content (0–0.07%) did not affect the crystal structure of the BCZT ceramics. It is clear however that the tetragonality of the sintered samples increased with increase in the concentration of CeO_2. The cell parameters established by Rietveld refinement are listed in Table 1. We do not have the direct evidence of the orthorhombic phase in the XRD analysis as we obtained evidence from a temperature-dependent relative permittivity plot as discussed below. The reason is possibly the temperature at which the XRD measurement was conducted. We measured the XRD patterns at room temperature (21°C) while the orthorhombic-tetragonal (O-T) phase transition was found at around 32°C by the temperature dependent relative permittivity plot. Temperature dependent XRD measurement may therefore be conducted to analyze more precise phase identification which in future studies.

Figure 4(d) depicts the temperature dependent relative permittivity of BCZT-xCeO_2 ceramics measured at 1 kHz. All specimens undergo two-phase transitions, i.e. the orthorhombic-tetragonal phase transition (T_{O-T}) near 32°C and the tetragonal – cubic phase transition (T_C) at around 100°C. Similar results were obtained in our previous study [30]. A small amount of CeO_2 doping (x = 0.02–0.07%) did not change the crystal structure but significantly increased the relative permittivity (ε_r). The highest value for ε_r was observed as 15,067 for x = 0.07%, compared to 6659 found for x = 0%. The enhancement of relative permittivity may be attributed to the uniform grain sizes and highly dense microstructure caused by a small addition of CeO_2. T_C decreased slightly from ~103°C to nearly 96°C due to the compositional adjustment of Ce ions in the BCZT lattice. Moreover, the addition of CeO_2 led to a larger c/a ratio, as shown in Figure 5, which demonstrates that the tetragonality of these ceramics rises and phase boundary moves.

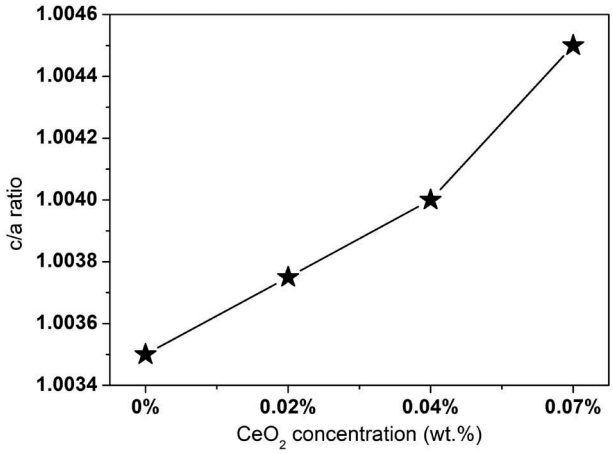

Figure 5. The c/a ratio as a function of the CeO_2 concentration at sintering conditions of T_1-1400°C/30 min & T_2-1275°C/4 h.

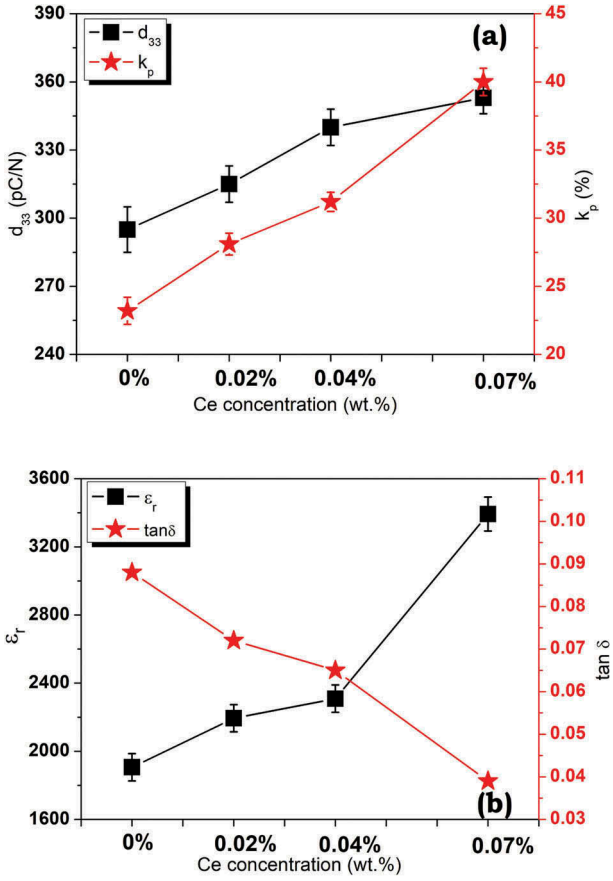

Figure 6. (a) The piezoelectric coefficient and planer coupling coefficient and (b) the relative permittivity and dissipation factor as functions of the Ce concentration at sintering conditions of T_1-1400°C/30 min & T_2-1275°C/4 h.

3.3. Piezoelectric and dielectric properties at room temperature

Figure 6(a,b) represents piezoelectric and dielectric properties of BCZT-xCeO_2 ceramics under sintering conditions of T_1-1400°C/30 min & T_2-1275°C/4 h. It can be clearly seen in Figure 6(a,b), that the planar coupling coefficient (k_p) and piezoelectric constant (d_{33}) increased with increase in the Ce concentration and achieved the maximum for the sample x = 0.07%, while the dissipation factor (tan δ) was reduced. The d_{33} was altered from 295 ± 15 pC/N of x = 0% to 353 ± 7 pC/N of x = 0.07% and the dissipation factor was reduced from 0.088 to 0.039 units. In addition, k_p increased from 23.2 ± 2% to 40 ± 1%, while relative permittivity increased from 1906 ± 80 to 3393 ± 100 at room temperature. This improvement in d_{33}, k_p, and ε_r

Table 2. Physical, piezoelectric and dielectric properties of BCZT-xCeO_2 ceramics at sintering conditions T_1-1400°C/30 min and T_2-1275°C/4 h.

BCZT – $_xCeO_2$	Relative density (g/cm^3)	Grain Size (μm)	d_{33} (pC/N)	K_p (%)	ε_r	T_C (°C)
x = 0	90.47 ± 0.05	8.0 ± 0.75	295 ± 15	23.2 ± 2	1906 ± 80	103.4
x = 0.02	91.51 ± 0.05	6.9 ± 0.29	315 ± 10	28.1 ± 1	2193 ± 80	100.1
x = 0.04	92.61 ± 0.05	7.24 ± 0.44	340 ± 10	28.9 ± 2	2308 ± 80	101.2
x = 0.07	99.00 ± 0.05	7.96 ± 0.71	353 ± 7	40 ± 1	3393 ± 100	96.2

Table 3. Ferroelectric properties of BCZT-xCeO_2 ceramics at sintering conditions T_1-1400°C/30 min and T_2-1275°C/4 h.

BCZT- $xCeO_2$ (in wt.%)	P_r (μC/cm^2)	P_{max} (μC/cm^2)	S_{max} (%)	E_C (kV/cm)
x = 0%	4.22	10.52	0.11	3.17
x = 0.02%	5.00	12.00	0.13	2.45
x = 0.04%	5.65	13.00	0.14	2.47
x = 0.07%	11.61	20.26	0.18	2.32

and the reduction in tan δ were ascribed to the final ceramic density and uniform grain sizes. The piezoelectric and dielectric properties are summarized in Table 2. Previously, CeO_2 was used as an additive to PZT and BNBT materials [35,36], and it generally showed some effects on enhancing d_{33} and reducing tan δ at the same time. CeO_2 showed the same double effect here. The mechanism of CeO_2 on BCZT ceramics is more complex and is described in our previous study in detail [30]. Moreover, Ce ions possibly exist in two valance states, i.e. Ce^{3+} of the ionic radius 0.13 nm and Ce^{4+} of the ionic radius 0.087 nm. In view of the ionic radius, Ce^{3+} obviously cannot enter the B site of the BCZT perovskite structure but can occupy the A site. Thus, there are two possible cases: Ce^{3+} can enter either the Ca^{2+} position (ionic radius = 0.134 nm) or the Ba^{2+} position (ionic radius = 0.161 nm). If it occupies the Ca^{2+} site, the replacement of Ca^{2+} by Ce^{3+} does not cause deformation (due to the fact that the ionic radius of both ions are nearly the same) in the BCZT lattice to make an evident contribution to increasing the domain movement. If Ce^{3+} occupies Ba^{2+} (ionic radius = 0.161 nm) on the other hand, then Ce^{3+} may act as a donor dopant leading to some cation vacancies at the A site, which may facilitate domain wall movement in order to enhance the piezoelectric properties of BCZT ceramics. By contrast, Ce^{4+} has a smaller ionic radius (0.087 nm) compared to Ce^{3+} and can possibly occupy the B-site of either Ti^{4+} (0.060 nm) or Zr^{4+} (0.072 nm). When the CeO_2 concentration is low as in our case, the occupation by Ce^{4+} of the Ti^{4+} site cannot lead to O-vacancies and therefore does not explain the dissipation factor decrease by O-vacancy mechanism. Kolar et al. previously explained the Ce^{3+} and Ce^{4+} effects on $BaTiO_3$ solid solutions in detail [37]. They presented the basis for showing the possibility that one of the few cases that the Ce^{3+} donor charge could be compensated by a reduction of Ti^{4+} to Ti^{3+} (electronic compensation) by creation of ionizing vacancies at the Ti sites or by a combination of both mechanisms [38,39]. This results in suppressing the movement of domains that cause a reduction in the dissipation factor (tan δ) [40].

3.4. Ferroelectric properties at room temperature

All ceramics show a polarization-electric (P-E) field loop as well as a current-electric field loop at sintering conditions of T_1-1400°C & T_2-1275°C, as depicted in Figure 7(a–d). For pure BCZT (x = 0%) a small remnant polarization (P_r = 4.22 μC/cm^2) is observed with a relatively large coercive field (E_C) of 3.17 kV/cm. As the Ce content increased up to x = 0.07%, a large remnant polarization (P_r = 11.61 μC/cm^2) with a low E_C = 2.32 kV/cm was observed. A low E_C suggest a soft nature of these ceramics, which indicates that Ce^{3+} acts as a donor dopant. The high P_r, may be attributable to large internal polarizability and large electromechanical coupling [41]. In addition, a sharp loop squareness generally indicates better homogeneity of grain sizes [41] as can be seen in Figure 7(d). Furthermore, I-E plot depicted in Figure 7(a–d), shows the switching process of these ceramics. For pure BCZT (x = 0%), the current peak intensity is low and broad, which indicates that the domain switching was not easy. A further increase in the Ce concentration (x = 0.02, 0.04%) provides some improvement in the current peak behavior and a sharp current peak was observed for the sample x = 0.07%. The width of the current peak gives the value of E_C at which remnant polarization could be obtained for ceramics [42,43]. Figure 8 represents the electric field induced strain loops for these ceramics. For sample x = 0.07%, a large strain (~0.18%) was observed under a 4 kV/mm positive electric field as compared to that of pure BCZT (x = 0%) as 0.11%. Such high bipolar strain values in a soft piezoelectric material may be attributable to easy domain motion. The ferroelectric properties are summarized in Table 3.

4. Conclusions

In this study, A sub-10 μm grain size and high-density (99%) uniform microstructure were obtained while maintaining good ferroelectric, dielectric and piezoelectric properties for BCZTCe ceramics via a two-step sintering technique. It has been reported that with TSS, grain size can be controlled (~8 μm) with a uniform microstructure. Addition of a small amount of CeO_2

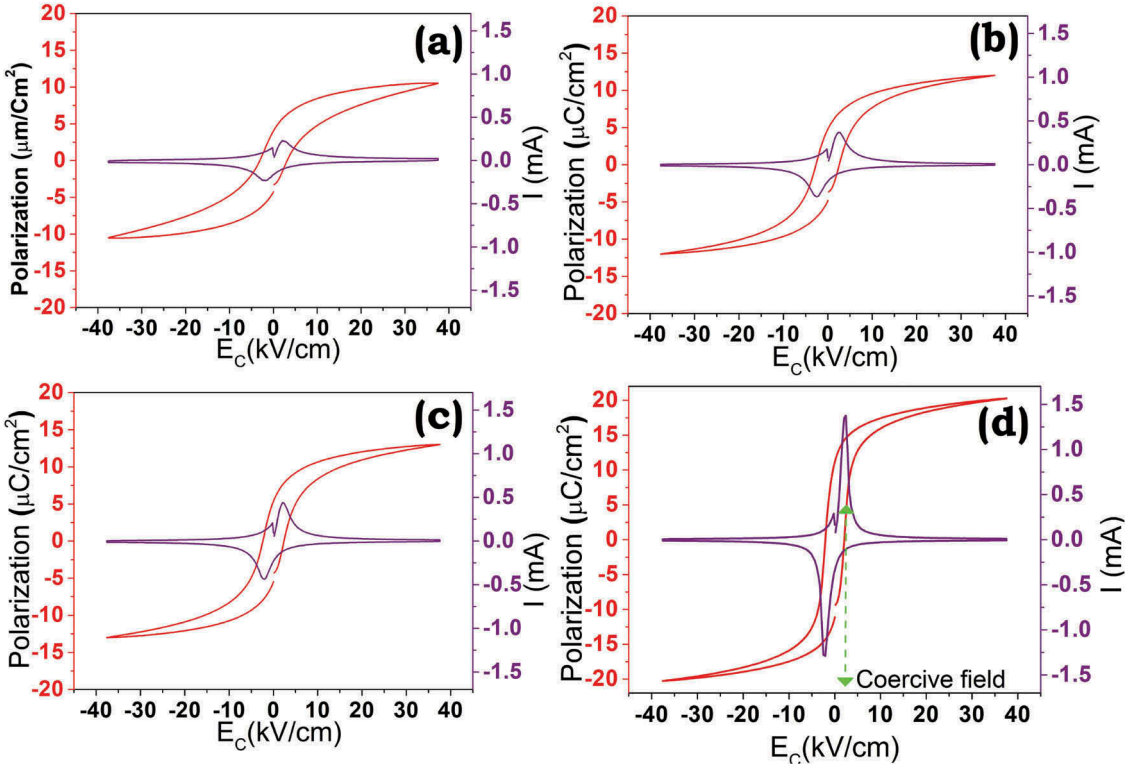

Figure 7. P-E hysteresis and I-E hysteresis responses for BCZT-xCeO_2 ceramics (a) x = 0% (b) x = 0.02% (c) x = 0.04% and, (d) x = 0.07% at sintering conditions of T_1-1400°C/30 min & T_2-1275°C/4 h.

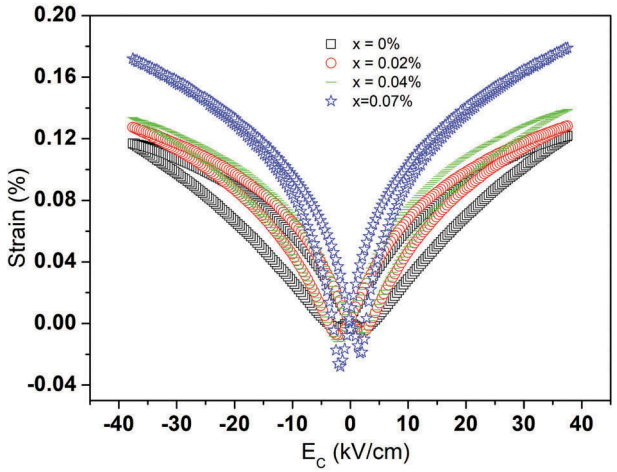

Figure 8. S-E curve for BCZT-xCeO_2 (x = 0–0.07 wt.%) ceramics at sintering conditions of T_1-1400°C/30 min & T_2-1275°C/4 h.

significantly reduced the sintering temperature as well as helping densification (relative density ~99%) which led to maintenance of good properties potentially suited to the fabrication of technological devices. The optimal properties were obtained for x = 0.07 wt.% at sintering conditions of T_1 = 1400°C & T_2 = 1275°C/4 h, in which d_{33} = 353 ± 7 pC/N, k_p= 40%, ε_r= 3393 ± 100, *tan* δ =0.039, T_C = 96.5°C, P_r = 11.45 μC/cm^2 and E_C = 2.32 kV/cm with an average *grain size* ~7–8 μm. These results strongly suggest that TSS is an effective sintering method for grain-size reduction with a uniform microstructure and that CeO_2 is a suitable dopant for reducing the sintering temperature as well as achieving enhanced density of BCZT ceramics.

Acknowledgments

The authors wish to acknowledge financial support from the Czech Ministry of Education within the framework of the National Sustainability Program under grant No. L01401 and the Grant Agency of the Czech Republic under grant No. 18-20498S. We further acknowledge CEITEC Nano RI, MEYS CR, 2016-2019, Czech Republic, for allowing the SEM and XRD measurements as well as the Advanced Materials Unit, CEITEC, for the use of laboratory facilities.

Disclosure statement

No potential conflict of interest was reported by the authors.

Funding

This work was supported by the Grantová Agentura České Republiky [18-20498S] and Czech Ministry of Education under Grant No. L01401.

ORCID

Vijay Bijalwan http://orcid.org/0000-0003-2858-5736

References

[1] Jaffe B, Cook WR, Jaffe H. Piezoelectric ceramics. New York: Academic Press; 1971.
[2] Saito Y, Takao H, Tani T, et al. Lead free piezoceramics. Nature. 2004;432:84–87.

[3] Damjanovic D, Klein N, Li J, et al. What can be expected from lead free piezoelectric materials? Funct Mater Lett. 2010;3:5–21.

[4] Rodel J, Jo W, Klaus TP, et al. Perspective on the development of lead free piezoceramics. J Am Ceram Soc. 2009;92:153–177.

[5] Lui W, Ren X. Large piezoelectric effect in Pb free ceramics. Phys Rev Lett. 2009;103:257602.

[6] Coondoo I, Panwar N, Amorn H, et al. Synthesis and characterization of lead free 0.5Ba $(Zr_{0.2}Ti_{0.\ 8})O_3$-$0.5(Ba_{0.\ 7}Ca_{0.\ 3})TiO_3$ ceramic. J Appl Phys. 2013;113:214107.

[7] Zhanga Q, Suna H, Wangb X, et al. Strong photoluminescence and piezoelectricity properties in Pr-doped $Ba(Zr_{0.2}Ti_{0.8})O_3$–$(ba_{0.7}Ca_{0.3})TiO_3$ ceramics: influence of concentration and microstructure. J Eur Ceram Soc. 2014;34:1439–1444.

[8] Ye SK, Fuh JY, Lu. L. Structure and electrical properties of 〈001〉 textured $(Ba_{0.85}Ca_{0.15})(Ti_{0.9}Zr_{0.1})O_3$ lead-free piezoelectric ceramics. Appl Phys Lett. 2012;100:252906.

[9] Qiao S, Wu J, Wu B, et al. Effect of $Ba_{0.85}Ca_{0.15}T_{i0.90}Zr_{0.10}O_3$ content on the microstructure and electrical properties of $Bi_{0.51}(Na_{0.82}K_{0.18})_{0.50}TiO_3$ ceramics. Ceram Int. 2012;38:4845–4851.

[10] Wu J, Wu W, Xiao D, et al. (Ba, Ca)(Ti, Zr)O_3 - $BiFeO_3$ lead free piezoelectric ceramics. Curr App Phys. 2012;12:534–538.

[11] Yueming L, Zugui X, Zongyang S, et al. Effect of BCZT on the properties of KNLNTS lead free piezoceramics. Rar Metall Mater Eng. 2013;42:175.

[12] Acosta M, Novak N, Rojas V, et al. $BaTiO_3$-based piezoelectrics: fundamentals, current status, and perspectives. Appl Phys Rev. 2017;4:041305.

[13] Ye S, Fuh J, Lu L, et al. Structure and properties of hot-pressed lead-free $Ba_{0.85}Ca_{0.15}Zr_{0.1}Ti_{0.9}O_3$ piezoelectric ceramics. RSC Adv. 2013;3:20693.

[14] Tian Y, Li S, Sun S, et al. Influence of europium doping on various electrical properties of low-temperature sintered $0.5Ba_{0.90}Ca_{0.10}TiO_3$ $0.5BaTi_{0.88}Zr_{0.12}O_3$-0.1%CuO-xEu lead-free ceramics. J Electron Mater. 2018;47:684–691.

[15] Wang P, Li Y, Lu Y. Enhanced piezoelectric properties $Ba_{0.85}Ca_{0.15}Zr_{0.1}Ti_{0.9}O_3$ lead-free ceramics by optimizing calcination and sintering temperature. J Eur Ceram Soc. 2011;31:2005–2012.

[16] Jin BM, Kim J, Kim SC. Effects of grain size on the electrical properties of $PbZr_{0.52}Ti_{0.48}O_3$ ceramics. Appl Phys A. 1997;65:53–56.

[17] Tang XG, Chan HL. Effect of grain size on the electrical properties of (Ba,Ca)(Zr,Ti)O_3 relaxor ferroelectric ceramics. J Appl Phys. 2005;97:034109.

[18] Payne DA, Frey MH. Grain-size effect on structure and phase transformations for barium titanate. Phys Rev B. 1996;54:3158–3169.

[19] Burfoot JC, Martirenat HT. Grain size effect on structure and phase transformations for barium titanate. J Phys C. 1974;7:3182–3192.

[20] Kiang C, Tan I, Ma J. Effects of LiF on the structure and properties of $Ba_{0.85}Ca_{0.15}Zr_{0.1}Ti_{0.9}O_3$ lead-free piezoelectric ceramics. Int J Appl Ceram Technol. 2013;10:701–706.

[21] Li W, Xu Z, Chu R, et al. Improved piezoelectric property and bright upconversion luminescence in Er doped $(Ba_{0.99}Ca_{0.01})(Ti_{0.98}Zr_{0.02})O_3$ ceramics. J Alloys Comp. 2014;583:305–308.

[22] Ma J, Liu X, Li W. High piezoelectric coefficient and temperature stability of Ga_2O_3-doped $(Ba_{0.99}Ca_{0.01})(Zr_{0.02}Ti_{0.98})O_3$ lead-free ceramics by low-temperature sintering. J Alloys Comp. 2013;581:642–645.

[23] Liu C, Liu X, Wang D, et al. Improving piezoelectric property of $BaTiO_3$–$caTiO_3$–$baZrO_3$ lead-free ceramics by doping. Ceram Int. 2014;40:9881–9887.

[24] Prasatkhetragarn A, Unruan M, Ngamjarurojana A, et al. Dielectric and ferroelectric properties of 0.8PZT–0.2PCN ceramics under sintering conditions variation. Curr App Phys. 2009;9:1165–1169.

[25] Cho J, Park I, Kim H, et al. Sintering behavior of cadmium doped $Pb(Ni_{1/3}Nb_{2/3})O_3$–$pbZrO_3$–$pbTiO_3$ ceramics. J Am Ceram Soc. 1997;80:1523–1534.

[26] Zheng P, Zhang JL, Tan YQ, et al. Grain-size effects on dielectric and piezoelectric properties of poled batio3 ceramics. Act Mater. 2012;60:5022–5030.

[27] Arlt G, Hennings D, de With G. Dielectric properties of fine-grained barium titanate ceramics. J Appl Phys. 1985;58:1619.

[28] Bijalwan V, Tofel P, Erhart J, et al. The complex evaluation of functional properties of nearly dense BCZT ceramics and their dependence on the grain size. Ceram Int. 2019;45:317–326.

[29] Zhu L, Zhang B, Zhao X, et al. Phase transition and high piezoelectricity in (Ba,Ca)(Ti1-xSnx)O3 lead-free ceramics. Appl Phys Lett. 2013;103:072905.

[30] Bijalwan V, Hughes H, Pooladvand H, et al. The effect of sintering temperature on the microstructure and functional properties of BCZT-$xCeO_2$ lead free ceramics. Mater Res Bull. 2019;114:121–129.

[31] Shrout T, Zhang S. Lead free piezoelectric ceramics. J Electroceram. 2007;9:113–126.

[32] Li J, Wang K, Zhang B, et al. Ferroelectric and piezoelectric properties of fine-grained $Na_{0.5}K_{0.5}NbO_3$ lead-free piezoelectric ceramics prepared by spark plasma sintering. J Am Ceram Soc. 2006;89:706–709.

[33] Castkova K, Maca K, Cihlar J, et al. Chemical synthesis, sintering and piezoelectric properties of $(Ba_{0.85}Ca_{0.15}Zr_{0.1}Ti_{0.9})O_3$ ceramics. J Am Ceram Soc. 2015;98:2373–2380.

[34] Bai Y, Matousek A, Tofel P, et al. (Ba,Ca)(Zr,Ti)O_3 lead-free piezoelectric ceramics-the critical role of processing on properties. J Eur Ceram Soc. 2015;35:3445–3456.

[35] Lee BW, Lee EJ. Effects of complex doping on microstructural and electrical properties of PZT ceramics. J Electroceram. 2006;17:597–602.

[36] Wang X, Chan H, Choy C. Piezoelectric and dielectric properties of CeO_2-added $(Bi_{0.5}Na_{0.5})_{0.94}Ba_{0.06}TiO_3$ lead-free ceramics. Sol State Commun. 2003;25:395–399.

[37] Makovec D, Samardzija Z, Kolar D. Solid solubility of cerium in $BaTiO_3$. J Solid State Chem. 1996;123:30–38.

[38] Jonker GH, Havinga EE. The effect of foreign ions on the crystal lattice of barium titanate. Mater Res Bull. 1982;17:345–350.

[39] Chan HM, Harmer MP, Smyth DM. Compensating defects in highly donor doped $BaTiO_3$. J Am Ceram Soc. 1986;69(6):507.

[40] Shi J, Yang W. Piezoelectric and dielectric properties of CeO_2-doped $(Bi_{0.5}Na_{0.5})0.94Ba_{0.06}TiO_3$ lead-free ceramics. J Alloys Comp. 2009;472:267–270.

[41] Haertling G. Ferroelectric ceramics: history and technology. J Am Ceram Soc. 1999;82:97.

[42] Kumar A, Bhanu Prasad VV, James Raju KC, et al. Poling electric field dependent domain switching and piezoelectric properties of mechanically activated $(Pb_{0.92}La_{0.08})(Zr_{0.60}Ti_{0.40})O_3$. J Mater Sci: Mater Electron. 2015;26:3757–3765.

[43] Viola G, Saunders T, Wei X, et al. the contribution of electrical conductivity, dielectric permittivity and domain switching in ferroelectric hysteresis loops. J Adv Dielectr. 2011;1:107–111.